COBEM 2021 26th International Congress of Mechanical Engineering
ABCM Associação Brasileira de Engenharia e Ciências Mecânicas
November 22-26, 2021, Virtual Congress, Brazil

COB-2021-0652
CO-DESIGN OF THE PLANT AND CONTROLLER OF ACTIVE SUSPENSION SYSTEM USING SEQUENTIAL, ITERATIVE AND NESTED OPTIMIZATION STRATEGIES

Stefany Patricia Dutra
Alexandro Garro Brito
Federal University of Santa Catarina, Dona Francisca Street, 8300, Distrito Industrial, Joinville, Santa Catarina, Brasil.
stefanydutra@gmail.com
alexandro.brito@ufsc.br

Abstract. *This article presents a sequential, iterative and nested optimization strategies in automotive suspension systems, in order to improve the performance of the system in terms of ride comfort and vehicle safety. In this proposal it is intended to treat the elastic constant of the spring and the damping coefficient of the damper as dependent optimization variables, relating them through geometric constraints. The main contribution of this work is the realization of the co-design of automotive suspension systems considering parametric uncertainties in the parameters of the plant to obtain the robust controller of dynamic output feedback. The* H_∞ *control problem is formulated using linear matrix inequalities. The study is based on the quarter car model with two degrees of freedom. The performance of the co-design is evaluated by computer simulations and compared with an active design. The road irregularities are represented by the speed bump input. The vertical acceleration over the sprung mass is used to evaluate ride comfort, while the vehicle safety is measured through the contact force between the tire and the track. The simulation shows the effectiveness of the sequential, iterative and nested co-design methods and their advantage, in terms of optimizing of ride comfort and vehicle safety, compared to active design.*

Keywords: *automotive suspension, sequential strategy, iterative strategy, nested strategy, linear matrix inequalities.*

1. INTRODUCTION

The design of vehicle suspension systems is influenced by several of conflicting performance requirements. These requirements include isolating the passengers from vibrations and road disturbances in order to provide a good ride quality and the guarantee of good adherence to the road, keeping the wheels in contact with the ground when oscillations arising from irregularities and keeping them in a favorable position during the curves (Rajamani, 2006). Active suspensions can provide the trade-offs between these requirements as they have the capacity not only to store and dissipate energy, but also to modulate the flow and provide energy for the system (Alyaqout *et al*., 2012).

The conventional design of the active suspension system is based on design techniques of the parameters of the mechanical structure, followed by the control design, in order to improve the dynamic performance of the system (Wuwei and Qirui, 2003). The main disadvantage of solving these two problems in a conventional way is that it does not guarantee the complete optimization of the dynamic system (Patil *et al*., 2010). Thus, the conventional method does not guarantee the ideal coupling between the mechanical design and the control system, producing suboptimal results (Allison *et al*., 2014).

Design strategies that manage the coupling between the definition of the physical artifacts and the control system are being developed and are called co-design methods (Allison *et al*., 2014). This approach allows carrying out the project based on the balance between the performance of the mechanical structure and the controller. Thus, a co-design method of the mechanical structure and controller parameters allows the optimal values to be obtained (Wuwei and Qirui, 2003).

In recent years, the co-design of the mechanical structure and the controller has been applied to a wide variety of systems, ranging from active suspension systems (Fathy, Papalambros, Ulsoy and Hrovat, 2003), (Fathy, Papalambros and Ulsoy, 2003), (Alyaqout *et al*., 2012), (Allison *et al*., 2014), semi-active suspension systems (Wuwei and Qirui, 2003), (Deshmukh *et al*., 2015), transmission for electric vehicles (Hofman and Janssen, 2017) to advanced powertrain systems (Alexander *et al*., 2012).

According to Fathy (2003), there are several strategies for the plant and controller optimization project. The main strategies can be divided into four categories: sequential, iterative, nested and simultaneous strategies, as illustrated in Figure 1.

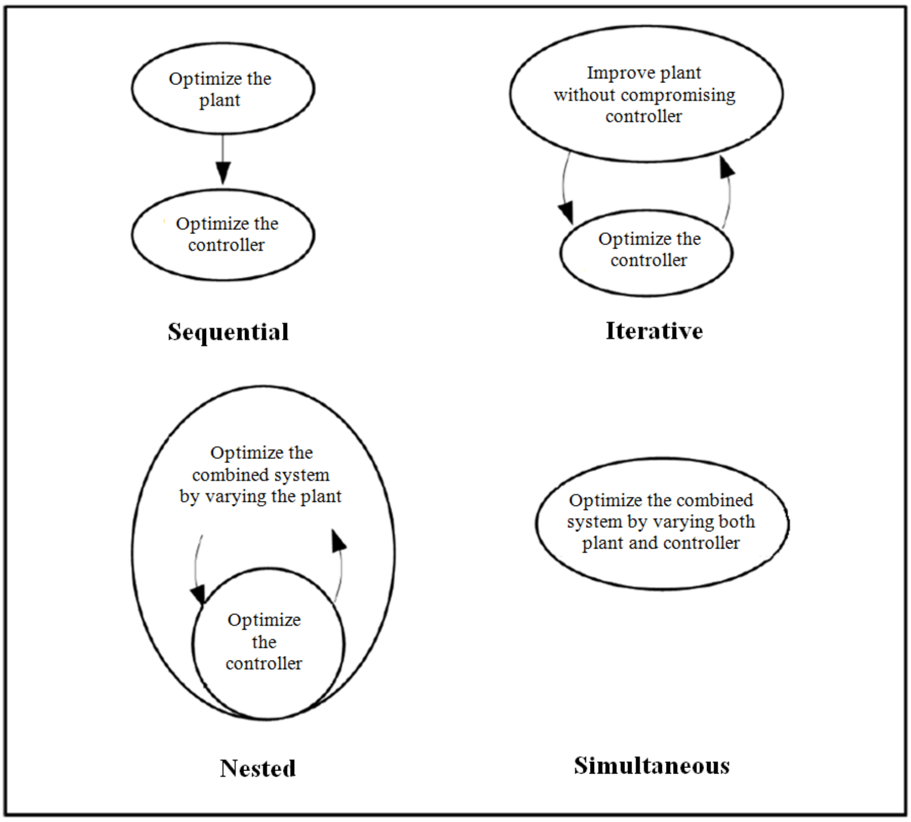

Figure 1. Plant and controller optimization strategies (Dutra, 2019).

The sequential strategy is the conventional approach to optimizing co-design problems, in which there are at least two separate optimization problems (Herber, 2014). In the sequential strategy the plant is optimized first. Once the plant design is completed, the design variables are treated as parameters in the controller design (Peters, 2010).

The iterative optimization strategy is solved iteratively by performing the artifact design first, without compromising the controller design. Next, the controller design is performed with the plant parameters frozen. This cycle takes place until convergence is reached.

The nested (or two-level) optimization strategy requires two optimization routines: an outer loop that solves the plant's optimal design problem and an inner optimization loop that identifies the optimal control for each plant design considered by the outer loop. The results of each iteration become the starting point for the next iteration, and this process is repeated until convergence (Peters, 2010).

Simultaneous co-design optimizes artifact and control variables in the same optimization formulation. That is, the simultaneous optimization algorithm tries to optimize a combined plant/controller objective function by varying the plant and controller designs simultaneously, subject to the combined set of plant and controller constraints (Fathy, 2003).

The objective of this work is to implement the sequential, iterative and nested co-design methods to improve the performance of the active suspension. This study intends to treat the elastic constant of the spring and the damping coefficient of the damper as dependent optimization variables, relating them through geometric constraints. In this way, the aim is to show the improvements that, even so, this project provides in relation to the conventional project. Differently from other works, the article is focused on identifying more real and appropriate parameters for the construction of the spring and the damper of the active suspension.

2. VEHICLE SUSPENSION MODEL

The suspension dynamics is based on in the quarter car model, represented by a linear system of two degrees of freedom, as shown in Figure 2. In this model, the sprung mass represents a quarter of the total vehicle body mass and the unsprung mass represents the axle-wheel assembly. The suspension system is composed of a spring with constant elastic k_s in parallel with a shock absorber with damping coefficient b_s. The active control force F_A is applied between the two masses by means of an actuator. The tire's elastic constant is called k_t. The two degrees of freedom of the model are represented by the vertical displacement of the sprung mass Z_s and the vertical displacement of the unsprung mass Z_u. The disturbance Z_r is caused by runway irregularities (Dutra, 2016).

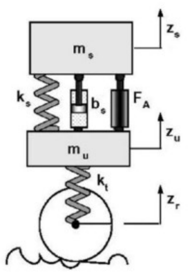

Figure 2. Quarter car model (Dutra, 2016).

The dynamic model of the system can be described by

$$\dot{\boldsymbol{x}}(t) = \boldsymbol{A_p}\boldsymbol{x}(t) + \boldsymbol{B_A}\boldsymbol{F_A}(t) + \boldsymbol{B_r}\boldsymbol{Z_r}(t), \tag{1}$$

where $\boldsymbol{x}$ is the state vector, defined by

$$\begin{bmatrix} \boldsymbol{x_1}(t) \\ \boldsymbol{x_2}(t) \\ \boldsymbol{x_3}(t) \\ \boldsymbol{x_4}(t) \end{bmatrix} = \begin{bmatrix} \boldsymbol{Z_s} - \boldsymbol{Z_u}(t) \\ \dot{\boldsymbol{Z}}_s - \dot{\boldsymbol{Z}}_u(t) \\ \boldsymbol{Z_u}(t) \\ \dot{\boldsymbol{Z}}_u(t) \end{bmatrix}, \tag{2}$$

where $\boldsymbol{x_1}(t)$ is the vertical displacement between sprung mass and unsprung mass, $\boldsymbol{x_2}(t)$ is the vertical velocity between sprung mass and unsprung mass, $\boldsymbol{x_3}(t)$ is the vertical displacement of the unsprung mass and $\boldsymbol{x_4}(t)$ is the vertical velocity of the unsprung mass. And the matrices $\boldsymbol{A_p}$, $\boldsymbol{B_A}$ and $\boldsymbol{B_r}$ are given by

$$\boldsymbol{A_p} = \begin{bmatrix} 0 & 1 & 0 & 0 \\ -k_s\left(\frac{1}{m_s} + \frac{1}{m_u}\right) & -b_s\left(\frac{1}{m_s} + \frac{1}{m_u}\right) & \frac{k_t}{m_u} & 0 \\ 0 & 0 & 0 & 1 \\ \frac{k_s}{m_u} & \frac{b_s}{m_u} & \frac{k_t}{m_u} & 0 \end{bmatrix}, \tag{3}$$

$$\boldsymbol{B_A} = \begin{bmatrix} 0 & \left(\frac{1}{m_s} + \frac{1}{m_u}\right) & 0 & -\frac{1}{m_u} \end{bmatrix}^T, \tag{4}$$

$$\boldsymbol{B_r} = \begin{bmatrix} 0 & -\frac{k_t}{m_u} & 0 & \frac{k_t}{m_u} \end{bmatrix}^T. \tag{5}$$

The parameters k_s and b_s have been treated as independent design variables in many co-design works (Fathy, Papalambros, Ulsoy and Hrovat, 2003), (Verros *et al*., 2005), but it is known that, in fact, depend on the geometric design and constraints. Here, based on the study by (Allison *et al*., 2014), k_s and b_s are treated as dependent variables through geometric constraints. A plant model is used that calculates the elastic constant and the damping coefficient as a function of the independent geometric variables of the spring and damper design.

2.1 Spring design

Figure 3 illustrates a helical compression spring with square ends and one end fixed to the ground. The coil spring encloses the damper, which is coaxial.

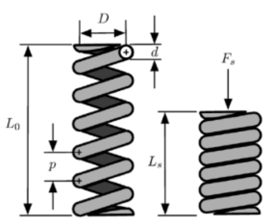

Figure 3. Helical compression spring (Allison *et al*., 2014).

The free spring length L_o and the solid spring length L_s are given, respectively, by:

$$L_o = pN_a + 2d, \tag{6}$$

$$L_s = p(N_a + 3), \tag{7}$$

where p is the spring pitch and N_a is the number of active coils.

The stiffness coefficient of the suspension spring is given by (Allison *et al.*, 2014):

$$k_s = \frac{d^4 G}{8D^3 N_a\left(1+\frac{1}{2C^2}\right)}, \tag{8}$$

where d is the wire diameter, G is the shear modulus of the material, D is the helix diameter and $C=D/d$ is the spring index, which is a measure of the curvature of the turn. According to Shigley, Mischke and Budynas (2003), for most coil springs C is in the range of 4 to 12. These requirements provide the first two plant design constraints (x_p):

$$f_1(x_p) = 4 - C \leq 0, \tag{9}$$

$$f_2(x_p) = C - 12 \leq 0. \tag{10}$$

As a way to guarantee the absolute stability of the spring, that is, to avoid it's bending (Shigley, Mischke and Budynas, 2003):

$$f_3(x_p) = L_o - \frac{\pi D}{\alpha}\left[\frac{2(E-G)}{2G+E}\right]^{1/2} \leq 0, \tag{11}$$

where E is the modulus of elasticity of the material and $\alpha = 0{,}5$ for springs with square ends and one of the ends fixed to the ground.

The uncompressed spring must fit within the specified length L_{omax} for the vehicle:

$$f_4(x_p) = L_o - L_{o_{max}} \leq 0. \tag{12}$$

The inner diameter and outer diameter of the spring are defined, respectively, as:

$$D_{int} = D - d, \tag{13}$$

$$D_{ext} = D + d. \tag{14}$$

With this definition, there is the restriction that the external diameter of the spring must not exceed the maximum allowable diameter D_{extmax} to avoid interference with the vehicle components:

$$f_5(x_p) = d + D - D_{ext_{max}} \leq 0. \tag{15}$$

Also, the inside diameter of the spring must be larger than the minimum allowable diameter D_{intmin} and large enough to fit around the damper with at least δ_{dc} of clearance. These requirements provide the restrictions given by Equations (16) and (17), respectively.

$$f_6(x_p) = D - d - D_{int_{min}} \geq 0, \tag{16}$$

$$f_7(x_p) = d - D + D_p + 2(\delta_{dc} + t_d) \leq 0. \tag{17}$$

In Equation (17), D_p is the diameter of the working piston of the damper and t_d is the thickness of the damper wall (Allison *et al.*, 2014).

2.2 Damper design

The project considers a single-tube telescopic damper, where linear damping is assumed, in which the damping force is proportional to the speed of the damper piston. The damper operating principle, its damping and thermal properties can be found in (Allison *et al.*, 2014).

The damping coefficient is given by:

$$b_s = \frac{D_p^4}{8C_d C_2 D_o^2}\sqrt{\frac{\pi k_v \rho_1}{2}} \, , \tag{18}$$

where k_v is the spool valve spring constant, ρ_1 is the damper fluid density, C_d is the discharge coefficient and C_2 is the damper valve coefficient, given by:

$$C_2 = \eta A_f \sqrt{x_m}. \tag{19}$$

The coefficient $0 < \eta < 1$ defines the upper limit of the proportion of the spool valve's outer circumference that can be exposed. The area factor $0 < A_f < 1$ is used to adjust the shape of the port and x_m is the maximum valve lift at the maximum allowable pressure in the damper, given by:

$$x_m = \frac{A_o P_{allow}}{k_v}. \tag{20}$$

The front area of the spool valve A_o is obtained by Equation (21) and the maximum pressure allowed in the damper P_{allow} is given by Equation (22).

$$A_o = \frac{\pi D_o^2}{4}, \tag{21}$$

$$P_{allow} = \frac{4 b_s V_{max}}{\pi D_p^2}, \tag{22}$$

where V_{max} is the maximum damper piston speed.

The damper stroke, which is the available axial displacement of the working piston, D_s is designated as an independent design variable.

To ensure that the shock fits within the specified length L_{omax} for the vehicle, the restriction is:

$$f_8(\boldsymbol{x}_p) = 2D_s + l_{d1} + l_{d2} - L_{o_{max}} \le 0, \tag{23}$$

where l_{d1} and l_{d2} quantify the space required for the shock components above and below the working piston range, respectively (Allison *et al.*, 2014).

3. SEQUENTIAL, ITERATIVE AND NESTED OPTIMIZATION STRATEGIES

In this section, the sequential, iterative and nested co-design methods of an active suspension system are presented. The optimization variables for the plant, which make up and the plant design vector x_p, are the wire diameter d, the helix diameter D, the spring pitch p, the working piston diameter D_p and the valve diameter D_o, and for the controller, the feedback gain vector $K(s)$.

Lower and upper limits are imposed on the plant design variables to prevent them from deviating from their typical values, and the mesh stability closed and imposed as a constraint on plant and controller projects (Fathy, Papalambros, Ulsoy and Hrovat, 2003).

When considering the uncertainty of the dynamic model of the suspension system, the H_∞ control is an appropriate tool to ensure stability or robust performance (Wuwei and Qirui, 2003). The H_∞ control consists of designing a controller such that the norm infinite of the transfer function between the exogenous input and the controlled output $T_{zw}(s)$ is minimal. And therefore a problem of rejecting disturbances, insofar as,

$$\|T_{zw}(s)\|_\infty = sup_{u(t)} \frac{\|z(t)\|_2}{\|w(t)\|_2}, \tag{24}$$

being that $\|w(t)\|_2 > 0$ (Vidyasagar, 1986).

The suspension system's goals are to isolate the vehicle's passengers from road disturbances in order to provide good ride quality and to produce continuous contact between the tire and the track to ensure good road holding. Therefore, in order to optimize driving comfort and vehicle safety, the H_∞ controller is designed to reduce the effect of road disturbances on the sprung mass and reduce the effect of road disturbances on tire deflection. In this case, as outputs to be controlled there is the vertical acceleration of the suspended mass $\ddot{Z}_s$ and the difference between the displacement of the unsprung mass and the irregularity of the track $Z_u - Z_r$. The suspension workspace, $Z_s - Z_u$, has also been added as a performance output. The control output used to feedback the system is the suspension workspace $Z_s - Z_u$.

3.1 Sequential optimization strategy

The sequential optimization strategy consists of optimizing the plant parameters and then optimizing the controller parameters. Given the initial design parameters of the plant, the initial controller is calculated. With this controller, given the initial conditions of the plant design parameters and the plant restrictions, the optimization of the plant parameters is performed (Dutra, 2019).

3.2 Iterative optimization strategy

The iterative optimization strategy consists of first carrying out the design of the plant parameters, without compromising the controller design. Next, the controller design is carried out with the plant parameters frozen. This cycle takes place iteratively until convergence is reached. Given the initial design parameters of the plant the initial controller is calculated. With this controller, given the initial conditions of the plant design parameters and the plant restrictions, the optimization of the plant parameters is performed. With the values of the plant parameters optimized, the H_∞ controller is optimized. This process is solved iteratively until convergence is reached or until the maximum number of iterations allowed by the user is reached (Dutra, 2019).

3.3 Nested optimization strategy

In the nested optimization strategy an external optimization loop executes the plant design and an internal optimization loop identifies the optimal control for each plant design tested by the external loop. This process is repeated until the system's optimized performance index is found. Given the initial design parameters of the plant, with the plant restrictions, the outer loop performs the optimization of the structure parameters. For the state model of structure of the plant, the inner loop designs the controller H_∞.The algorithm evaluates the cost or the minimum value found for $\|T_{zw}(s)\|_\infty$ and repeats this process until it finds the system's optimized performance index (Dutra, 2019).

4. ANALYSIS OF THE DYNAMICS OF THE SUSPENSION SYSTEM

In this section the simulation results are described. Since it has been accepted that an active suspension has better driving comfort and vehicle safety than a passive suspension, we pay more attention here to the comparisons between active suspension without co-design (active) and with co-design (sequential, iterative and nested).

The nominal data of the suspension were taken from Patole and Sawant (2015), with its parameters defined in Table 1.

Table 1. Vehicle parameters.

Parameters	Value	Units
Sprung mass (m_s)	515,45	kg
Unsprung mass (m_u)	23,61	kg
Suspension spring elastic constant (k_s)	12394	N/m
Tire elastic constant (k_t)	181818	N/m
Suspension damper damping coefficient (b_s)	1385	Ns/m

The nominal values of the helix diameter, the wire diameter and the number of active coils for the spring consists, respectively, of D = 0,12307 m, d = 0,012 m and N_a = 6. Specifying the spring free length L_{omax} = 0,330 m and using Equation (6), with the nominal values of d and N_a, we obtain p = 0,051 m.

The minimum inner diameter is defined as D_{intmin} = 0,071 m and the maximum outer diameter as D_{extmax} = 0,175 m. The spring design considers ASTM A401 steel, which has a modulus of elasticity E = 203,4 GPa and a shear modulus G = 77,2 GPa. According to Allison, Guo and Han (2014), a gap of δ_{dc} = 0,0090 m between spring and damper wall thickness to be t_d = 0,0020 m. The spring pitch is a relationship that depends on the wire diameter value.

In the design of the damper, the discharge coefficient is specified to be approximately C_d = 0,70 for spool valves, the spool valve spring constant k_v = 7500 N/m and the fluid density of the damper ρ_l = 850 kg/ m^3 (Allison *et al*., 2014).

The initial values referring to the spring design are selected as the nominal ones, D = 0,123 m, d = 0,012 m, p = 0,051 m. In relation to the initial values of the damper design, it is assumed D_p = 0,033 m and D_o = 0,0051 m, which corresponds to the average value of the lower and upper limit of each parameter. These parameters lead to k_s = 17837,080679 N/m and b_s = 1510,307857 Ns/m, according to Equations (8) and (18).

The design constraints referring to the suspension spring and damper are given by:

$$4d \leq D \leq 12d \, , \tag{25}$$

$$L_o \leq 5{,}26D, \tag{26}$$

$$L_o \leq 0{,}330, \tag{27}$$

$$d + D \leq 0{,}17, \tag{28}$$

$$D - d \geq 0{,}071\,, \tag{29}$$

$$d - D + D_p + 0{,}022 \leq 0, \tag{30}$$

$$3d \leq p \leq 6d, \tag{31}$$

$$0{,}030 \leq D_p \leq 0{,}036, \tag{32}$$

$$0{,}0042 \leq D_0 \leq 0{,}0061. \tag{33}$$

In this work, the optimization problems of the plant parameters were performed using the *fmincon* optimization function and the optimization problems of the controller were made through the *sdpt3* solver.

The optimized plant parameters for sequential, iterative and nested co-design are shown in Table 2.

Table 2. Optimized plant parameters for sequential, iterative and nested co-design.

Co-design	Sequential	Iterative	Nested
d (m)	0,00951225095365513	0,00976169356064154	0,00747710219388820
D (m)	0,0971338347899398	0,0915615463688901	0,0789421270052388
p (m)	0,0462858706150663	0,0434509361648377	0,0448481564592797
D_p (m)	0,0348929101384232	0,0351200543665258	0,0448481564592797
D_o (m)	0,00609808993838836	0,00609550655494245	0,00609966278675873
k_s (N/m)	12770,08162189458	15885,38268943090	8688,830132477528
b_s (Ns/m)	1169,736827139416	1202,021349465216	1108,071134735042

For a comparative analysis of the performance between the systems, the vehicle is considered passing through the bump excitation, 3,70 m long and 0,10 m high, at a speed of 30 km/h, as shown in Figure 4.

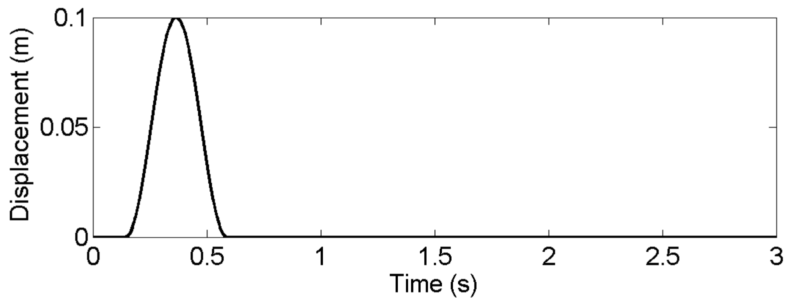

Figure 4. Bump excitation.

As comparison parameters are used the vertical acceleration of the sprung mass and the contact force between the tire and the track. The Figure 5(a) shows the behavior of the acceleration of the sprung mass for the active and sequential design, the Figure 5(b) shows the behavior of the acceleration of the sprung mass for the active and iterative design and the Figure 5(c) shows the behavior of the acceleration of the sprung mass for the active and nested design.

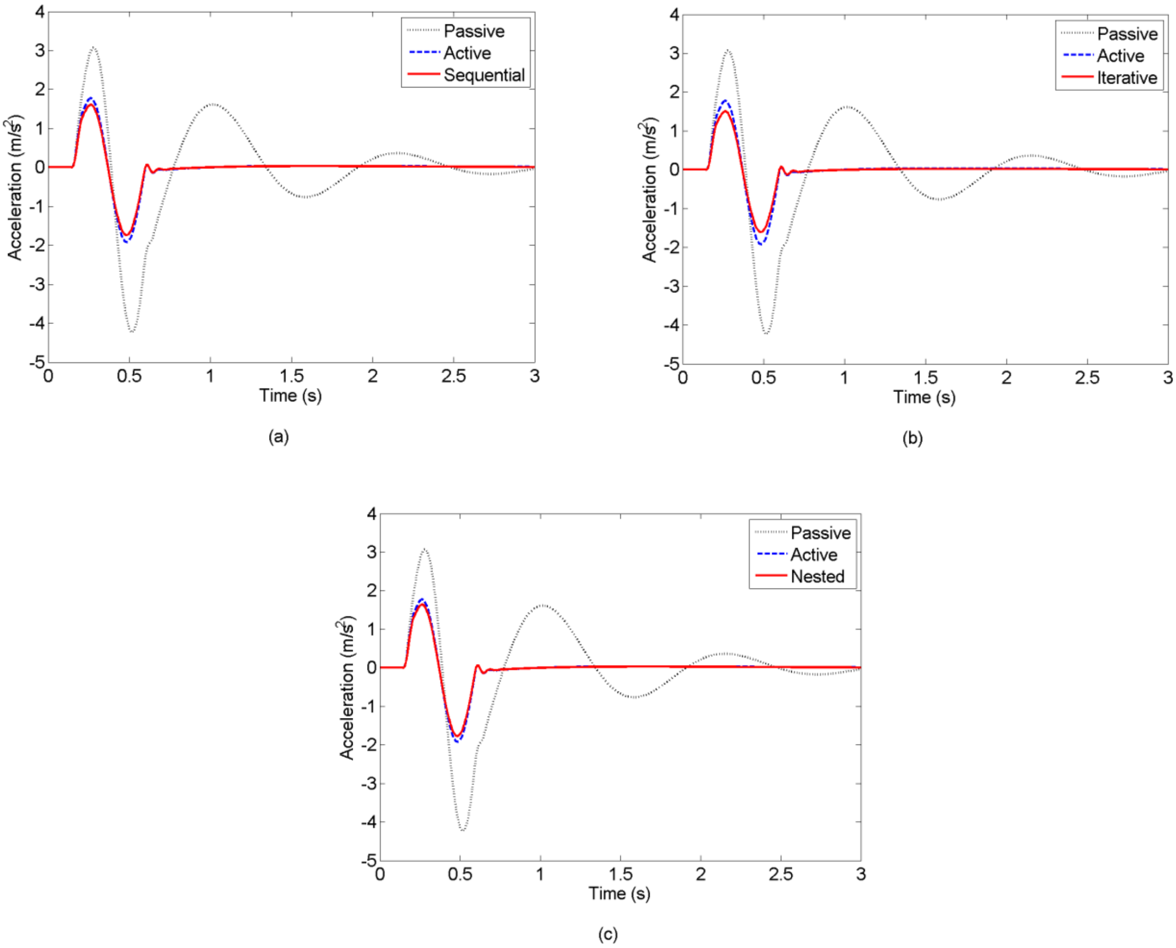

Figure 5. Sprung mass acceleration response for passive, active and in (a) for sequential design, in (b) for iterative design, and in (c) for nested design.

The Figure 6(a) shows the behavior of the contact force between tire and track for the active and sequential design, the Figure 6(b) shows the behavior of the contact force between tire and track for the active and iterative design and the Figure 6(c) shows the behavior of the contact force between tire and track for the active and nested design.

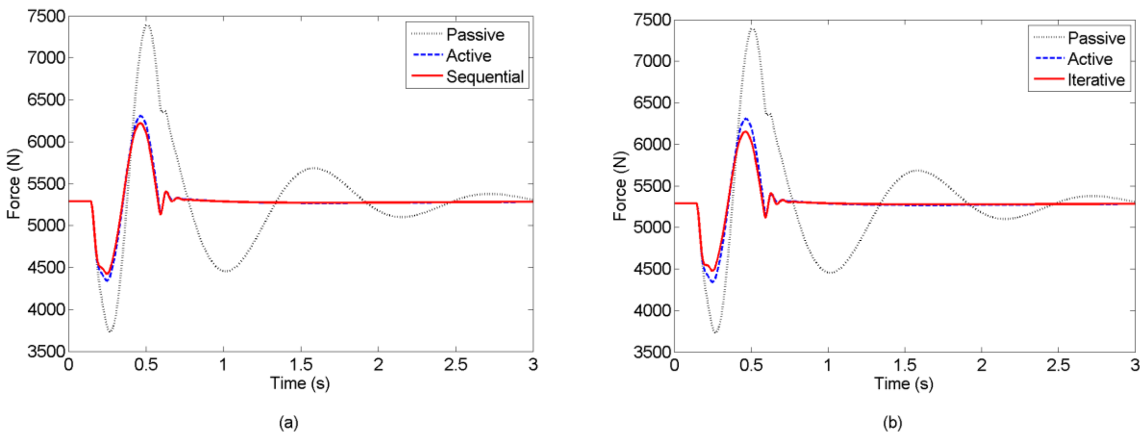

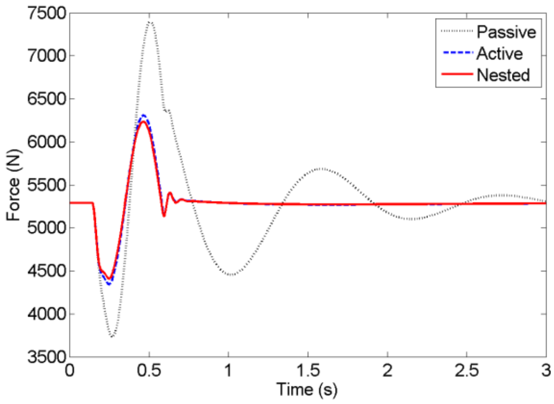

(c)

Figure 6. Contact force between tire and track for passive, active and in (a) for sequential design, in (b) for iterative design, and in (c) for nested design.

The Table 3 and Table 4 show, respectively, the values of the vertical acceleration of the sprung mass and the contact force between the tire and the track, for the active, sequential, iterative and nested systems.

Table 3. Sprung mass acceleration.

Acceleration [m/s^2]	Maximum	Minimum	RMS
Active	1,77	-1,91	0,50
Sequential	1,61	-1,74	0,45
Iterative	1,50	-1,60	0,42
Nested	1,64	-1,77	0,46

Table 4. Contact force between the tire and the track.

Force [N]	Maximum	Minimum
Active	6307,48	4342,30
Sequential	6219,58	4423,13
Iterative	6151,73	4475,33
Nested	6234,09	4407,77

It is verified that the sequential and nested system reduces by 7,14% the peak-to-peak value of the temporal response of the sprung mass acceleration and the iterative system reduces by 28,57% the peak-to-peak value of the temporal response of the sprung mass acceleration.

Regarding the contact force between the tire and the track, it can be seen that the sequential system reduces by 8,58% the peak-to-peak value of the temporal response, the iterative reduces by 14,69% the peak-to-peak value of the temporal response and the nested reduces by 7,06% the peak-to-peak value of the temporal response.

5. CONCLUSIONS

This article presented a sequential, iterative and nested approach for the co-design of the mechanical structure parameters and control parameters of active automotive suspension systems. The project was based on the quarter car model, using the controller whose objective was to minimize the effect of road disturbances on the sprung mass and minimize the effect of road disturbances on tire deflection, subject to the physical restrictions of the spring and shock absorber. Differently from other works, the optimization of constructive parameters of the suspension was investigated, instead of the suspension coefficients. This makes this project closer to practical reality.

In order to show the efficiency of the proposed sequential, iterative and nested co-design methods, a comparison of the performance of the active system with the sequential, iterative and nested system was presented. The systems were compared in relation to the temporal response of the movements that represent the comfort and safety of the vehicular system. Comfort was represented by the vertical acceleration of the sprung mass and vehicle safety by the force of contact between the tire and the road.

The results were satisfactory. Through the discussion elaborated in the previous section, it is possible to prove the efficiency of the sequential, iterative and nested co-design methods and its advantage, in terms of optimizing driving comfort and safety, in relation to the active project.

6. ACKNOWLEDGEMENTS

The authors thank CAPES for the financial assistance granted.

7. REFERENCES

Alexander, M.J., Allison, J.T., and Papalambros, P.Y, 2012. *"Decomposition–based design optimization of electric vehicle powertrains using proper orthogonal decomposition".* Int. Journal of Powertrains, Vol. 1, No. 1, pp. 72–92.

Allison, J.T., Guo, T., and Han, Z., 2014. *"Co–design of an active suspension using simultaneous dynamic optimization"*. Journal of Mechanical Design, Vol. 136, pp. 1–14.

Alyaqout, S.F., Papalambros, P.Y., and Ulsoy, A.G., 2012. "*Combined design and robust control of a vehicle passive/active suspension"*. Int. J. Vehicle Design, Vol. 59, No. 4, pp. 315-330.

Deshmukh, A.P., Herber, D.R., and Allison, J.T., 2015. *"Bridging the gap between open–loop and closed–loop control in co–design: a framework for complete optimal plant and control architecture design".* American Control Conference, pp. 4916–4922.

Dutra, S. P., 2016. *Controle H_∞ de sistemas de suspensão ativa veicular*. Trabalho de Conclusão de Curso (Graduação), Curso de Engenharia Automotiva, Universidade Federal de Santa Catarina, Joinville.

Dutra, S. P., 2019. *Projeto integrado de sistemas de suspensão ativa veicular*. Dissertação (Mestrado), Programa de Pós-graduação em Engenharia de Sistemas Eletrônicos, Universidade Federal de Santa Catarina, Joinville.

Fathy, H.K., 2003. *Combined plant and controller optimization: theory, strategies and applications*. Doctoral Thesis, Mechanical Engineering, University of Michigan, Ann Arbor.

Fathy, H.K., Papalambros, P.Y., and Ulsoy, A.G., 2003. *"Integrated plant, observer, and controller optimization with application to combined passive/active automotive suspensions".* ASME International Mechanical Engineering Congress and Exposition, Dynamic Systems and Control, Vol. 1,2, pp. 15–21.

Fathy, H.K., Papalambros, P.Y., Ulsoy, A.G., and Hrovat, D., 2003. *"Nested plant/controller optimization with application to combined passive/active automotive suspensions"*. American Control Conference, pp. 3375–3380.

Herber, D.R.,, 2014. *Dynamic system optimization of wave energy converters utilizing direct transcription.* Master Thesis, Science in Systems and Entrepreneurial Engineering, Graduate College of the University of Illinois at Urbana-Champaign, Urbana.

Hofman, T., and Janssen, N., 2017. *"Integrated design optimization of the transmission system and vehicle control for electric vehicles"*. Elsevier, Vol. 50, No. 1, pp. 10072–10077.

Patil, R., Filipi, Z., and Fathy, H., 2010. *"Computationally efficient combined design and control optimization using a coupling measure"*. IFAC Symposium on Mechatronic Systems. pp. 144–151.

Patole, S.S., and Sawant, S.H., 2015. "*Theoretical and numerical analysis of half car vehicle dynamic model subjected to different road profiles with wheel base delay and nonlinear parameters*". International Journal of Multidisciplinary and Current Research, Vol. 3, pp. 542–546.

Peters, D.L., 2010. *Coupling and controllability in optimal design and control.* Doctoral Thesis, Mechanical Engineering, University of Michigan, Ann Arbor.

Rajamani, R., 2006. *Vehicle dynamics and control*, New York: Springer.

Shigley, J., Mischke, C., and Budynas, R. 2003. *Mechanical engineering design*. New York: McGraw-Hill.

Verros, G., Natsiavas, S., and Papadimitriou, C., 2005. "*Design optimization of quarter–car models with passive and semi–active suspensions under random road excitation*", J. Vib. Control, Vol. 11, No. 5, pp. 581–606.

Vidyasagar, M., 1986. "*Optimal rejection of persistent bounded disturbances*". IEEE Trans. Automatic Control, Vol. 31, No. 6, pp.527–534.

Wuwei, C., and Qirui, W., 2003. *"Integrated design of structure/control systems of semi–active suspension using genetic algorithms and H_∞control scheme".* Int. J. Vehicle Autonomous Systems, Vol. 1, No. 3/4, pp. 387-404.

8. RESPONSIBILITY NOTICE

The author(s) is (are) the only responsible for the printed material included in this paper.